

The host of GRB/XRF 030528 – an actively star forming galaxy at $z = 0.782^*$

A. Rau, M. Salvato, and J. Greiner

Max-Planck-Institut für extraterrestrische Physik, Giessenbachstrasse, 85748 Garching, Germany
e-mail: arau@mpe.mpg.de

Received 6 July 2005 / Accepted 11 August 2005

ABSTRACT

An important parameter for the distinction of X-ray flashes, X-ray rich bursts and Gamma-ray bursts in the rest frame is the distance to the explosion site. Here we report on the spectroscopic redshift determination of the host galaxy of XRF/GRB 030528 using the ESO VLT FORS2 instrument. From the strong oxygen and hydrogen emission lines the redshift was measured to be $z = 0.782 \pm 0.001$. Obtaining the line luminosities and ratios we find that the host is consistent with being an actively star forming galaxy with sub-solar metallicity. With a stellar mass of $\sim 10^{10} M_{\odot}$ the host is placed among the most massive GRB host galaxies at a similar redshift. Estimating the redshifted properties of the prompt emission, we find that XRF/GRB 030528 would be classified as an X-ray rich burst in the rest frame rather than an X-ray flash in the typically-used observer frame.

Key words. gamma rays: bursts

1. Introduction

The distribution of observer frame peak energies in νF_{ν} , $E_{\text{peak}}^{\text{obs}}$, of the prompt high-energy emission of Gamma-ray bursts (GRBs) ranges from several keV up to a few MeV with a clustering around 250 keV (Preece et al. 2000). Recently, special attention was drawn to the extreme low energy part of the distribution. Based on *Beppo-SAX* Wide-Field Camera observations (Heise et al. (2001) classified these events as so-called X-ray flashes (XRFs). XRFs are similar to long duration GRBs in various prompt burst properties (e.g. the duration and the low and high-energy spectral slopes) but are characterized by $E_{\text{peak}}^{\text{obs}} \leq 30$ keV. An operational classification based on the ratio of X-ray to γ -ray fluence, $\log(S_X(2-30 \text{ keV})/S_{\gamma}(30-400 \text{ keV}))$ in the observer frame, was proposed for events detected by the *HETE-2* satellite (Sakamoto et al. 2004). According to this definition, one third of all *HETE-2*-localized bursts are X-ray flashes with $\log(S_X/S_{\gamma}) > 0$, another third are X-ray rich bursts (XRR) having $\log(S_X/S_{\gamma}) > -0.5$, with the rest being the “classical” GRBs (Lamb et al. 2005).

It has been suggested that XRFs represent the extension of GRBs to bursts with low peak energies and that XRFs, XRRs and GRBs form a continuum (Heise et al. 2001; Barraud et al. 2003). This was strengthened by the discoveries of X-ray (Harrison et al. 2001), optical (Soderberg et al. 2003) and radio (Taylor et al. 2001) afterglows for some XRFs with properties

similar to those found for GRBs. Furthermore, for XRF 020903 (Soderberg et al. 2005) and XRF 030723 (Fynbo et al. 2004) possible supernova bumps in the afterglow light curves have been reported similar to the observed associations of the deaths of massive stars with long-duration GRBs (e.g. Hjorth et al. 2003; Stanek et al. 2003; Zeh et al. 2004).

A variety of theoretical models has been proposed to explain the observed peak energies of XRFs. E.g., (i) a high baryon loading in the GRB jets can result in bulk Lorentz factors much smaller than those expected in GRBs (Dermer et al. 1999; Huang et al. 2002); (ii) similarly, a low contrast between the bulk Lorentz factors of the colliding relativistic shells can produce XRF-like events (Barraud et al. 2005); (iii) for GRB jets which are not pointed directly at the observer the spectrum will be softer as well (Yamazaki et al. 2002); (iv) the peak energies of GRBs at high redshift will be moved to lower energies and can mimic XRFs in the observer frame (Heise et al. 2001).

An important discriminator between the individual models is the distance scale to the explosion site. A number of XRFs have been localized to arcminute accuracy in the past but only for a few could accurate distances be obtained so far. For XRF 020903 and 030429 the redshift could be measured unambiguously as $z = 0.251$ (Soderberg et al. 2004) and $z = 2.66$ (Jakobsson et al. 2005), respectively. A third event, XRF 040701, has a candidate host galaxy at $z = 0.2146$ (Kelson et al. 2004) associated with one of the two tentatively fading X-ray sources in the error box (Fox 2004). For some

* Based on observations collected at the European Southern Observatory, La Silla and Paranal, Chile under ESO Program 075.D-0539.

more XRFs, upper limits on the redshift could be set from optical follow-up observations. In two cases, XRF 011030 and 020427, host galaxies with typical properties of GRB hosts have been detected and photometric evidence suggests the redshifts to be $z < 3.5$ (Bloom et al. 2003) and $z < 2.3$ (van Dokkum & Bloom 2003), respectively. For XRF 030727 a firm upper limit of $z = 2.3$ could be placed from the absence of Ly α absorption and prominent lines in the afterglow spectrum as well as from a light curve bump associated with possible underlying supernova (Fynbo et al. 2004).

Here we report on the spectral analysis of the host galaxy of GRB/XRF 030528. After summarizing the known properties of the burst and host (Sect. 2) we present the observations and data reduction (Sect. 3). The obtained host properties derived from the spectrum are shown in Sect. 4 and the implications in the context of XRFs and GRB/XRF host galaxies are discussed in Sect. 5.

We use a cosmology of $\Omega_m = 0.27$, $\Omega_\Lambda = 0.7$ and $H_0 = 70 \text{ km s}^{-1} \text{ Mpc}^{-1}$ throughout the paper. All photometric magnitudes are given in the AB system.

2. GRB/XRF 030528

The high energy transient was detected by *HETE-2* as a long-duration Gamma-ray burst (HETE trigger #2724)¹. The event was moderately bright with a fluence of $S = 5.6 \pm 0.7 \times 10^{-6} \text{ erg cm}^{-2}$ and a peak flux on a one second time scale of $4.9 \times 10^{-8} \text{ erg cm}^{-2} \text{ s}^{-1}$ in the 30–400 keV band (Sakamoto et al. 2005). The burst duration (given as T_{90} , which is the time over which a burst emits from 5% of its total measured counts to 95%) was $T_{90} = 49.2 \pm 1.2 \text{ s}$ (30–400 keV) and the high energy spectrum peaked at $32 \pm 5 \text{ keV}$. With $\log(S_X/S_\gamma) = 0.04$, the event was classified as an X-ray flash. Accordingly, we will refer to the event as XRF 030528 throughout this paper, while in other places (e.g. Butler et al. 2004; Rau et al. 2004, R04 hereafter) the identifier GRB 030528 was used.

The burst occurred in a crowded field of the sky near the Galactic Plane (LII = 0°:0462 & BII = 11°:2902) which lead to complication of the ground based optical follow-up observations by a significant Galactic foreground extinction. A faint near-IR afterglow was detected (Greiner et al. 2003) and at the same position a fading X-ray source was found with *Chandra* (Butler et al. 2003).

In R04 we described the properties of the near-IR afterglow as well as a photometric study of the detected underlying host galaxy. The galaxy was found to be among the brightest observed GRB hosts with $K_{AB} \sim 21.8 \pm 0.7 \text{ mag}$. A fitting of template spectral energy distributions (SEDs) to the photometry in *V*, *R*, *I*, *J*, *H* and *K* showed that the host properties were consistent with that of a young star forming galaxy. Unfortunately, the lack of spectroscopy and the sparse photometric sampling of the SED did not allow us to determine the redshift accurately, but the data favor $z < 1$.

3. Observations and data reduction

The host galaxy of XRF 030528 was observed with the Focal Reducer and low-dispersion Spectrograph 2 (FORSS2) at the 8.2 m ESO Very Large Telescope (VLT) Antu in Paranal, Chile. Twelve exposures, each lasting 594 s, were taken in two nights, on Apr. 12, 2005 and May 6, 2005. We obtained longslit spectroscopy using the 300 V grism together with the order separation filter GG435, thus covering a spectral range of approx. 5200–9200 Å. Using a 1''0 slit, the $3.3 \text{ \AA pixel}^{-1}$ scale leads to a resolution of 13.5 \AA (*FWHM*) at 1''0 seeing.

Flat-field, bias correction and cosmic ray removal was applied in the standard fashion using IRAF². The wavelength calibration of the combined spectra was done using HgCdHe+Ar calibration lamps. The standard star LTT 7379 (spectral type G0) was used for the flux calibration of the spectra. In addition a correction for telluric absorption was performed using an observation of the telluric standard star EG 274 (spectral type DA).

Using the far-IR extinction maps of Schlegel et al. (1998) the Galactic foreground extinction in the direction of XRF 030528 is estimated as $E(B - V) = 0.62$. Several authors have argued that the far-IR analysis overestimates the value of $E(B - V)$ by up to ~30% for fields at low galactic latitude. Dutra et al. (2003) suggest a rescaling of the Schlegel et al. extinction by 0.75 which results in an $E(B - V) = 0.46$ for the line of sight towards the host of XRF 030528. For the following analysis we corrected the spectra according to the rescaled value and consider this as a lower limit of the foreground extinction. All presented spectral parameters (line fluxes and luminosities) and absolute magnitudes have to be considered as lower limits.

4. Results

The final summed spectrum of the host galaxy is shown in Fig. 1. A number of significant emission lines are detected which we identified as [OII] ($\lambda 3727 \text{ \AA}$), H β ($\lambda 4861 \text{ \AA}$), [OIII] ($\lambda 4959 \text{ \AA}$) and [OIII] ($\lambda 5007 \text{ \AA}$) at a helio-center corrected redshift of $z = 0.782 \pm 0.001$. This corresponds to a luminosity distance of $D_L = 4.949 \pm 0.008 \text{ Gpc}$ using the cosmological parameters given above. At this redshift H β and the [OIII] emission lines coincide with prominent sky emission features which complicates the accurate extraction of the line properties and effects possible weak detections of H γ and H δ in emission. Only [OII] falls into a wavelength range empty of sky features.

We measured the emission line strengths using a Gaussian fit in IRAF *splot*. The line fluxes are listed in Table 1 together with the estimated redshifts and the according line luminosities. The widths of the emission lines are consistent with the instrumental line width (560 km s^{-1} at $\lambda = 7000 \text{ \AA}$) and do not show signs of intrinsic broadening. Consistent with the photometric measurements in the *V*, *R* and *I* bands presented in

¹ <http://space.mit.edu/HETE/Bursts/Data>

² IRAF is distributed by the National Optical Astronomy Observatories, which are operated by the Association of Universities for Research in Astronomy, Inc., under cooperative agreement with the National Science Foundation.

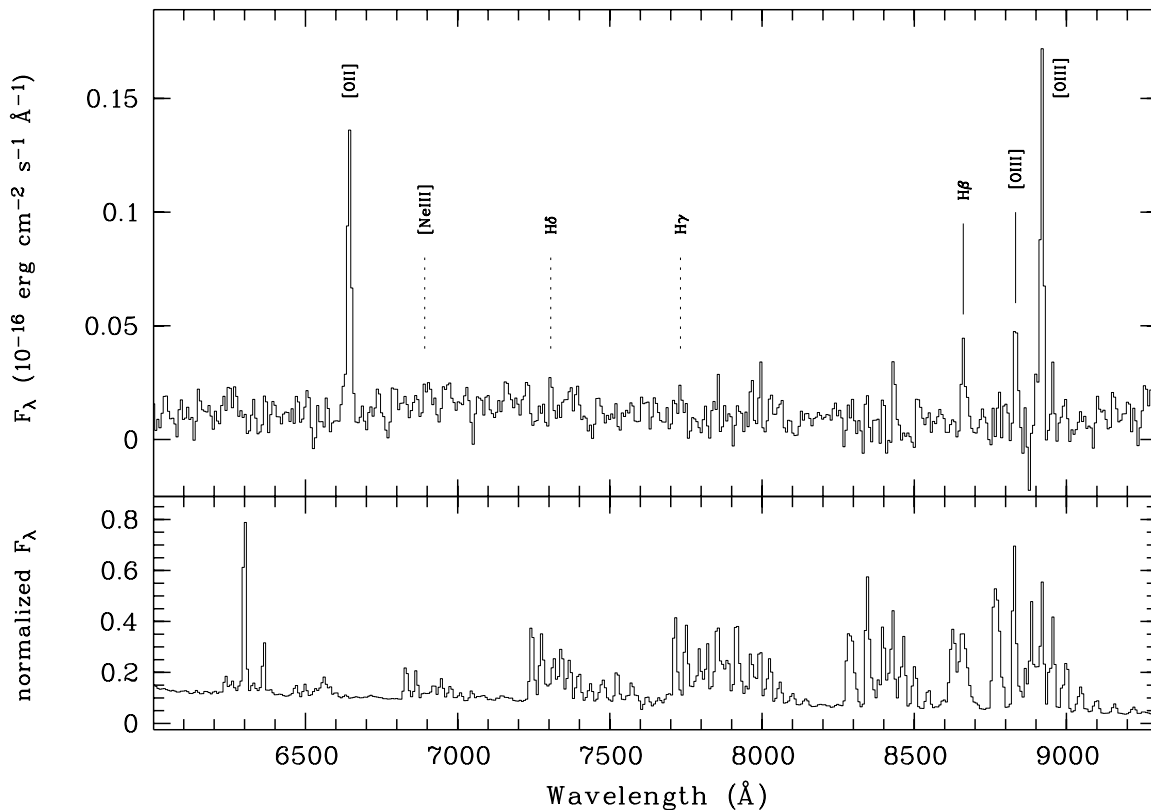


Fig. 1. *Top:* final FORS2 long-slit spectrum of the host galaxy with an exposure of ~ 2 h. The positions of the identified emission lines (solid lines) and a selection of undetected lines (dashed) are indicated. The host continuum is only marginally detected. Residuals of sky emission features are visible above 8000 \AA . *Bottom:* normalized sky spectrum showing the prominent telluric emission lines.

Table 1. Line identifications. Columns: observer frame wavelengths λ_{obs} , corresponding emission line redshifts z , line fluxes and corresponding luminosities for the lines indicated in the spectrum shown in Fig. 1. Note that we do not apply a correction for underlying Balmer absorption.

Line	λ_{obs} \AA	z	Flux	
			$10^{-17} \text{ erg/s/cm}^2$	L 10^{41} erg/s
[OII] $\lambda 3727$	6644	0.783	15 ± 1	4.4 ± 0.2
[NeIII] $\lambda 3869$	6891	0.781	< 1	< 0.3
H δ $\lambda 4102$	7306	0.781	< 2.5	< 0.7
H γ $\lambda 4340$	7732	0.781	< 2.5	< 0.7
H β $\lambda 4861$	8661	0.782	4.8 ± 0.4	1.4 ± 0.2
[OIII] $\lambda 4959$	8833	0.781	4 ± 1	1.2 ± 0.3
[OIII] $\lambda 5007$	8919	0.781	20 ± 1	5.9 ± 0.3

R04, the host continuum is only marginally traced. The resulting uncertainty in the continuum flux prevents us from deriving sensitive equivalent widths for the lines.

The spectrum is uncorrected for possible intrinsic extinction in the host galaxy. In order to get an estimate of the extinction we used the Balmer line ratios and fits to the spectral energy distribution using the host photometry presented in R04. Due to the shift of H α to the near-IR only the ratios of H γ /H β and H δ /H β can be used to estimate $E(B - V)$. Comparing the line ratios derived from the strict upper limits of the line fluxes for H γ and H δ with the theoretical values

(Brocklehurst 1971) we find that no constraints for the extinction can be obtained. In an independent attempt we applied SED fitting to the broad-band photometry in V, R, I, J_s, H and K using HyperZ (Bolzonella et al. 2000) and theoretical spectral model templates of Bruzual & Charlot (1993). The sparse photometric sampling of the host together with the considerable uncertainties provides lower and upper limits of $A_V = 0$ and $A_V = 2.5$, respectively ($\chi^2 < 1$). Thus, only a lower limit of the intrinsic extinction $A_V = 0$ can be derived. Therefore, the line strengths given in Table 1 have to be considered as strict lower limits.

The unextincted star formation rate (SFR) can be derived from the luminosity of the [OII] emission line, e.g. using the typical applied calibration of Kennicutt (1998, K98 hereafter), $SFR (M_\odot \text{ yr}^{-1}) = 1.4 \pm 0.4 \times 10^{-41} L_{[\text{OII}]}$. Taking the measured line luminosity as a lower limit for the real luminosity we estimate the unextincted star formation to be $> 6 \pm 2 M_\odot \text{ yr}^{-1}$. A measure for the extinction corrected SFR was proposed by Rosa-Gonzalez et al. (2002, RG02 hereafter), $SFR (M_\odot \text{ yr}^{-1}) = 8.4 \pm 0.4 \times 10^{-41} L_{[\text{OII}]}$. They derived “unbiased” SFR expressions, e.g. computed from the [OII] line luminosity and the UV continuum. Correcting for the effects of underlying stellar Balmer absorption their SFR estimators bring into agreement the rates measured with different indicators, including the far-IR. According to this calibrator we derive an extinction-corrected SFR of $37 \pm 4 M_\odot \text{ yr}^{-1}$.

The UV continuum directly probes the emission from young massive stars and thus is another measure of the

Table 2. Star formation rates and specific star formation rates for different indicators (Col. 1: [OII] and UV continuum at 2800 Å) and calibrators (Col. 2: Kennicutt 1998 and Rosa-Gonzalez et al. 2002). The derived SFRs are given in Col. 3 and the Cols. 4 and 5 show the specific SFRs for an $L_{\star,B}$ galaxy and per unit solar mass, respectively.

		<i>SFR</i>	Specific <i>SFR</i>	
		[$M_{\odot} \text{ yr}^{-1}$]	[$M_{\odot} \text{ yr}^{-1}$]	[$M_{\odot} \text{ yr}^{-1} M_{\odot}^{-1}$]
[OII]	K98	6 ± 2	12 ± 3	2×10^{-10}
	RG02	37 ± 4	74 ± 6	1.2×10^{-9}
UV	K98	4 ± 1	8 ± 2	1×10^{-10}
	RG02	17 ± 3	34 ± 4	5×10^{-10}

unextincted fraction of the ongoing star formation. The optimal rest frame wavelength (1500–2800 Å) lies outside of our spectroscopic coverage ($>2950 \text{ \AA}$ at $z = 0.782$), and the continuum is only marginally traced. Therefore, we used the best fitting SED to derive the flux at rest frame 2800 Å. The resulting lower limit for the UV *SFR* is $4 \pm 1 M_{\odot} \text{ yr}^{-1}$ when applying the K98 estimator, $SFR (M_{\odot} \text{ yr}^{-1}) = 1.4 \pm 0.4 \times 10^{-28} L_{\nu,UV}$, and $17 \pm 3 M_{\odot} \text{ yr}^{-1}$ for the corresponding extinction corrected calibrator of RG02, $SFR (M_{\odot} \text{ yr}^{-1}) = 6.4 \pm 0.4 \times 10^{-28} L_{\nu,UV}$. For clarity, the results are summarized in Table 2. The derived star formation rates are about a factor of two lower than the corresponding values obtained using the [OII] emission line as an indicator, which is fully consistent with the spread generally obtained when using various SFR indicators (e.g. Hopkins et al. 2001).

The metallicity of the host galaxy can be derived from the emission line indicator $R_{23} = \log([OII] + [OIII])/H\beta$ (Pagel et al. 1979). This empirical indicator is not unique and typically provides a double branch solution. This degeneracy can generally be broken using other strong emission lines (e.g. [NII] $\lambda 6584 \text{ \AA}$). For the host of XRF 030528 these lines are not available but the value of R_{23} falls onto the turnover of the two branches. Using the calibrations compiled in McGaugh (1991) we find $12 + [\log(O/H)] = 7.7\text{--}8.5$, which corresponds to a metallicity of 0.1–0.6 solar.

Knowing the redshift we determined the absolute magnitudes and luminosities of the host galaxy in various photometric bands. The rest frame absolute magnitudes (AB system, K-correction only) were derived using spectral template fitting in HyperZ with the intrinsic extinction fixed to zero. The resulting magnitudes are shown in Table 3 together with the respective magnitudes of an L_{\star} galaxy in a Schechter distribution function and the luminosities of the host in units of L/L_{\star} .

The host galaxy is of the order of L_{\star} in the *U*-band and subluminal at longer wavelengths, as expected for an actively star forming galaxy. Note that the use of the Schlegel et al. extinction value ($E(B - V) = 0.62$) without the correction suggested by Dutra et al. (see above) would affect mainly the bands shortwards of the rest frame *B*-band (roughly corresponding to the observer frame *R*). The corresponding luminosities for $E(B - V) = 0.62$ are $L_U \sim 2.2L_{\star,U}$ and $L_B \sim 0.9L_{\star,B}$, both a factor of two brighter than the results for $E(B - V) = 0.43$.

Table 3. Absolute magnitudes of the host galaxy in various photometric bands (AB system) together with the absolute magnitudes of an L_{\star} galaxy in a Schechter distribution function and the luminosity of the host in units of L/L_{\star} . Values for $M_{\star} - 5 \log h_{70}$ obtained for a range in redshift consistent with the redshift of our host galaxy were adopted from Dahlen et al. (2005) (*U, B, R_c* and *J*) and Cowie et al. (1996) (*K*). The uncertainties in *M* and L/L_{\star} do not contain the uncertainty in the Galactic reddening (see Sect. 3)

Rest frame band pass	<i>M</i>	$M_{\star} - 5 \log h_{70}$	L/L_{\star}
	[mag]	[mag]	
<i>U</i>	-20.5 ± 0.1	-20.3 ± 0.1	1.2 ± 0.2
<i>B</i>	-20.7 ± 0.1	-21.4 ± 0.1	0.5 ± 0.1
<i>R_c</i>	-21.1 ± 0.1	-22.3 ± 0.1	0.35 ± 0.05
<i>J</i>	-21.4 ± 0.1	-23.0 ± 0.2	0.25 ± 0.05
<i>K_s</i>	-21.6 ± 0.1	-23.5 ± 0.2	0.17 ± 0.05

Therefore, the magnitudes and luminosities given in Table 3 have to be understood as lower limits.

In addition to the star formation rate and luminosities we can also derive an estimate of the stellar mass in the host galaxy applying various methods. Using the correlation between the mass and rest frame *B* and *V*-band magnitudes of Bell et al. (2005), assuming a Kroupa (2001) initial mass function, we estimate the mass to be $\sim 2 \times 10^{10} M_{\odot}$. As the correlation assumes a wide range in stellar ages the obtained masses of galaxies with recent starburst activity, like the host of XRF 030528, will be overestimated. Nevertheless, the obtained mass is of the same order as the stellar mass derived from the rest frame *K*-band mass-to-light ratio of 0.8 (Brinchmann & Ellis 2000) of $\sim 9 \times 10^9 M_{\odot}$.

Using the luminosity of the host and its stellar mass the specific star formation rate in units of $M_{\odot} \text{ yr}^{-1}$ for an $L_{\star,B}$ galaxy and per unit mass can be estimated. The specific star formation rates for the RG02 *SFR* calibrators are 74 ± 6 and $34 \pm 4 M_{\odot} \text{ yr}^{-1}$ for an $L_{\star,B}$ galaxy derived from the [OII] and UV estimators, respectively and 1.2×10^{-9} and $5 \times 10^{-10} M_{\odot} \text{ yr}^{-1} M_{\odot}^{-1}$, respectively (see also Table 2).

5. Discussion

Accurate distance measurements for extragalactic high-energy transients like XRFs, XRRs and GRBs are important to discriminate between the proposed theoretical models and for the application of the events as cosmological probes. While the redshift distribution of classical GRBs now contains ~ 50 events covering a redshift range from $z = 0.0085$ to $z = 4.511$, the distance scale of XRFs is much less determined. The redshift measurement of XRF 030528 presented here gives the third secure distance to an XRF obtained so far and shows that XRFs, classified according to the *HETE-2* X-ray to γ -ray fluence ratio in the observer frame, cover a range consistent with that of the classical GRBs (Fig. 2).

A possible scenario associates XRFs with GRBs at high redshift (Heise et al. 2001). The three obtained XRF distances indicated that this can not be true for at least some of the events. Nevertheless, the shift of the rest frame peak energy to lower values in the observer frame cannot be neglected.

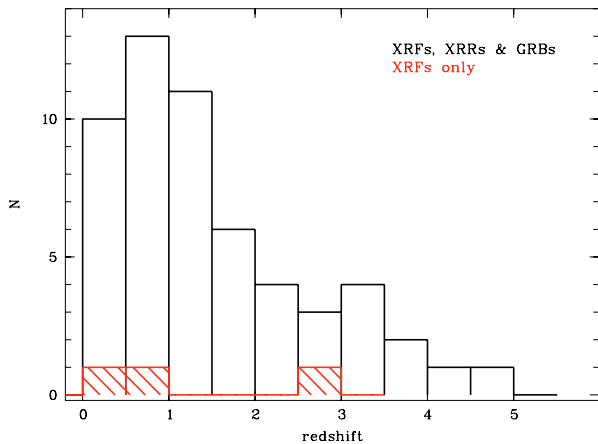


Fig. 2. Distribution of accurately measured redshifts for XRFs, XRRs and GRBs together (empty histogram) and XRFs only (hatched). The total sample contains 55 bursts with GRB 050803 (Bloom et al. 2005) being the latest entry. The XRFs are 020903, 030528 and 030429 at $z = 0.251$, 0.782 and 2.66 , respectively.

For XRF 030528 the observer frame peak energy of $E_{\text{peak}}^{\text{obs}} = 32 \pm 5$ keV corresponds to $E_{\text{peak}}^{\text{rest}} = 57 \pm 9$ keV at a redshift of $z = 0.782$. We modeled the high energy spectrum of the burst using a Band function (Band et al. 1993) with parameter values given for XRF 030528 in Sakamoto et al. (2005) and classified it according to the *HETE*-2 scheme in the rest frame. The obtained value of $\log(S_X/S_\gamma) \sim -0.17$ demonstrates that XRF 030528 would be defined as an X-ray rich burst at its rest frame rather than an XRF.

A similar estimate was obtained for XRF 030429 ($z = 2.66$). For this event $E_{\text{peak}}^{\text{obs}} = 35_{-8}^{+12}$ keV (Sakamoto et al. 2005) shifts to $E_{\text{peak}}^{\text{rest}} = 128_{-30}^{+43}$ keV in the rest frame. This corresponds to $\log(S_X/S_\gamma) \sim -0.43$ which places the burst at the borderline between “classical” GRBs and XRRs. From the three XRFs with accurately known redshift only for XRF 020903 ($E_{\text{peak}}^{\text{rest}} = 6$ keV) does its classification remain that of an XRF also in the rest frame. However, this event was especially soft and the physical similarity to bursts like XRF 030528 or 030429 is uncertain.

As shown above, the identification of bursts based on observer frame fluence ratios is in most cases only an operational classification. Naturally, a more sophisticated separation would need to be based on rest frame rather than observer frame properties. Nevertheless, it becomes increasingly evident that XRFs, XRRs and GRBs form a continuum of objects, a situation that questions the necessity of such a classification of events (both in the observer and in the rest frame) and evaluates it purely operationally.

Knowing the redshift, the isotropic equivalent energy for the prompt emission of XRF 030528 can be determined to be $E_{\text{iso},\gamma} = 2.0 \pm 0.7 \times 10^{52}$ erg in the 2–400 keV observer frame energy range. Together with $E_{\text{peak}}^{\text{rest}} = 57$ keV, XRF 030528 falls at the lower end of the correlation of $E_{\text{iso},\gamma}$ and $E_{\text{peak}}^{\text{rest}}$ (Lloyd-Ronning & Ramirez-Ruiz 2002; Amati et al. 2002). Assuming the validity of the relationship between $E_{\text{peak}}^{\text{rest}}$ and the collimation-corrected total energy, E_γ , proposed by Ghirlanda et al. (2004), the collimation fraction of the burst can be

estimated. Equation (3) of Ghirlanda et al. (2004) gives $E_\gamma = 4.8 \pm 0.7 \times 10^{49}$ for $E_{\text{peak}}^{\text{rest}} = 57$ keV. This implies a collimation factor of 2.4×10^{-3} and an opening angle of 4° , which is in the typical range for GRB jets (Frail et al. 2001).

The principal aim of the observation presented here was the estimation of the redshift of XRF 030528 and thus the further establishment of the distance scale of XRFs. XRF 030528 is no longer an XRF but an XRR in the rest frame. The good quality of the spectroscopic data provided us with the possibility to study also the underlying host galaxy in more detail. From the rest frame UV continuum and the [OII] emission line luminosity star formation rate, values ranging from 4 to $37 M_\odot \text{ yr}^{-1}$ were obtained. Despite the large uncertainty of the estimate, we can conclude that the host galaxy exhibits a significant level of ongoing star formation, similar to what was found by Christensen et al. (2004) in a sample of 10 GRB host galaxies.

XRF 030528 occurred in a galaxy which appears sub-luminous in the near-IR ($\sim 0.2 L_{\star,K}$) and rest-frame optical bands ($\sim 0.5 L_{\star,B}$). This is also typical for the hosts of long-duration GRBs studied so far (e.g., Sokolov et al. 2001; le Floc’h et al. 2003; Christensen et al. 2004). Furthermore, the gas in the host was found to be of sub-solar metallicity ($0.1\text{--}0.6 z$) using the emission line indicator R_{23} , in agreement with a recent study of three low- z GRB host galaxies by Sollerman et al. (2005). This suggests that the host of XRF 030528 is indeed an actively star forming galaxy as emphasized in R04.

Only a small number of estimates for the stellar mass content in GRB host galaxies have been performed so far (e.g. Sokolov et al. 2001; Chary et al. 2002). For the host of XRF 030528 we obtained the stellar mass using two independent indicators applied to the absolute magnitudes derived from the photometry presented in R04. Both methods gave consistent results of $M \sim 10^{10} M_\odot$, which places the host among the most massive GRB hosts at a similar redshift. Note that the previous mass estimates were obtained using synthesis model fitting while we used indicators based directly on the absolute B and V and K -band magnitudes.

At a redshift of $z = 0.782$, the angular extent of the host galaxy ($\sim 1''.5$; R04) corresponds to a linear size of ~ 11 kpc (ignoring possible inclination effects). This indicates that the host is not a dwarf galaxy but is more comparable in size with a spiral galaxy like the Milky Way.

The comparison of the specific star formation rate and the stellar mass of the host galaxy with galaxies in the FORS Deep Field and GOODS-South field at similar redshift shows that it falls into the group of young actively star forming galaxies (Feulner et al. 2005). This indicates once more (e.g., Bloom et al. 2003; Soderberg et al. 2004; Fynbo et al. 2004) that XRFs are associated with star forming regions in the universe as are GRBs and again suggests the similarity between these events. Unfortunately, the sparse afterglow and host photometry prevents us from deriving an accurate constraint on a supernova associated with XRF 030528. The obtained K -band brightness 14.8 days post-burst provides an upper limit for the absolute magnitude of any supernova of $K = -21.6$ mag, around 2 mag

brighter than most luminous core-collapse supernova observed in the near-IR (Mannucci et al. 2003).

While the indications that in many properties XRFs, XRRs and GRBs form a continuum in many properties are increasingly evident, the origin of the soft spectral peak in XRFs is not revealed for all events. In the case of XRF 030528 we showed that the classification in the observer frame differs from that obtained in the rest frame. At least in XRF 020903, the only “real” XRF with a known distance so far, this is not true. In order to distinguish between the individual models and to estimate the rest frame properties of the events accurately, redshift measurements for XRFs are still very important. These require accurate localizations which will be provided by the ongoing *HETE-2* mission as well as, with a lower rate, by the *Swift* instruments. Nevertheless, the detection of very soft events like XRF 020903 at high redshift ($z > 1$) will require sensitive instruments at even lower energies.

Acknowledgements. This work is based on observations collected at the European Southern Observatory, Chile, under proposal 075.D-0539. We thank D. Hartmann & S. Savaglio for the fruitful discussions. We thank the anonymous referee for valuable comments.

References

- Amati, L., Frontera, F., Tavani, M., et al. 2002, *A&A*, 390, 8
- Band, D., Matteson, J., Ford, L., et al. 1993, *ApJ*, 413, 281
- Barraud, C., Olive, J.-F., Lestrade, J. P., et al. 2003, *A&A*, 400, 1021
- Barraud, C., Daigne, F., Mochkovitch, R., & Atteia, J.-L. 2005, *A&A*, 440, 809
- Bell, E. F., Papovich, C., Wolf, C., et al. 2005, *ApJ*, 625, 23
- Bloom, J. S., Fox, D., van Dokkum, P. G., et al. 2003, *ApJ*, 599, 957
- Bloom, J. S., Perley, D., Foley, R., et al. 2005, *GCN*, 3758
- Bolzonella, M., Miralles, J.-M., Pello, R. 2000, *A&A*, 363, 476
- Brinchmann, J., & Ellis, R. S. 2000, *ApJ*, 536, L77
- Brocklehurst, M. 1971, *MNRAS*, 153, 471
- Bruzual, G., & Charlot, S. 1993, *ApJ*, 405, 538
- Butler, N., Dullighan, A., Ford, P., et al. 2003, *GCN*, 2279
- Butler, N., Dullighan, A., Ford, P., et al. 2004, in *Proc. Gamma-Ray Bursts: 30 Years of Discovery: Gamma-Ray Burst Symposium*, ed. E. E. Fenimore, & M. Galassi, AIPC, 727, 435
- Chary, R., Becklin, E. E., & Armus, L. 2002, *ApJ*, 566, 229
- Christensen, L., Hjorth, J., & Gorosabel, J. 2004, *A&A*, 425, 913
- Cowie, L. L., Songaila, A., Hu, E. M., & Cohen, J. G. 1996, *AJ*, 112, 389
- Dahlen, T., Mobasher, B., Somerville, R. S., et al. 2005, *ApJ*, 631, 126
- Dermer, C. D., Chiang, J., & Böttcher, M. 1999, *ApJ*, 513, 656
- Dutra, C. M., Ahumada, A. V., Claria, J. J., Bica, E., & Barbuy, B. 2003, *A&A*, 408, 287
- Feulner, G., Gabasch, A., Salvato, M., et al. 2005, *ApJL*, submitted
- Fox, D. B. 2004, *GCN*, 2630
- Frail, D. A., Kulkarni, S. R., Sari, R. et al. 2001, *ApJ*, 562, L55
- Fynbo, J. P. U., Sollerman, J., Hjorth, J., et al. 2004, *ApJ*, 609, 962
- Ghirlanda, G., Ghisellini, G., & Lazzati, D. 2004, *ApJ*, 616, 331
- Greiner, J., Rau, A., & Klose, S. 2003a, *GCN*, 2271
- Harrison, F. A., Yost, S., Fox, D. B., et al. 2001, *GCN*, 1143
- Heise, J., in ‘t Zand, J., Kippen, R. M., & Woods P. M. 2001, in *Gamma-Ray Bursts in the Afterglow Era*, ed. E. Costa, F. Frontera, & J. Hjorth (Berlin: Springer), 16
- Hjorth, J., Sollerman, J., Møller, P., et al. 2003, *Nature*, 423, 847
- Hopkins, A. M., Connolly, A. J., Haarsma, D. B., & Cram, L. E. 2001, *AJ*, 122, 288
- Huang, Y. F., Dai, Z. G., & Lu, T. 2002, *MNRAS*, 332, 735
- Jakobsson, P., Hjorth, J., Fynbo, J. P. U., et al. 2004, *A&A*, 427, 785
- Kelson, D. D., Koviak, K., Berger, E., & Fox, D. B. 2004, *GCN*, 2627
- Kennicutt, R. C. 1998, *ARA&A*, 36, 189
- Lamb, D. Q., Donaghy, T. Q., & Graziani, C. 2005, *ApJ*, 620, 355
- le Floch, E., Duc, P.-A., Mirabel, I. F., et al. 2003, *A&A*, 400, 499
- Lloyd-Ronning, N. M., & Ramirez-Ruiz, E. 2002, *ApJ*, 576, 101
- Mannucci, F., Maiolino, R., Cresci, G., et al. 2003, *A&A*, 401, 519
- McGaugh, S. S. 1991, *ApJ*, 380, 140
- Pagel, B. E. J., Edmunds, M. G., Blackwell, D. E., et al. 1979, *MNRAS*, 255, 325
- Preece, R. D., Briggs, M. A., Malozzi, R. S., et al. 2000, *ApJS*, 126, 19
- Rau, A., Greiner, J., Klose, S., et al. 2004, *A&A*, 427, 815
- Rosa-Gonzalez, D., Terlevich, E., & Terlevich, R. 2002, *MNRAS*, 332, 283
- Sakamoto, T., Lamb, D. Q., Graziani, C., et al. 2004, *ApJ*, 602, 875
- Sakamoto, T., Lamb, D. Q., Kawai, N., et al. 2005, *ApJ*, 629, 311
- Schlegel, D. J., Finkbeiner, D. P., & Davis, M. 1998, *ApJ*, 500, 525
- Soderberg, A. M., et al. 2003, *AAS Meet.* 203, 132.07
- Soderberg, A. M., Kulkarni, S. R., Berger, E., et al. 2004, *ApJ*, 606, 994
- Soderberg, A. M., Kulkarni, S. R., Fox, D. B., et al. 2005, *ApJ*, 627, 877
- Sollerman, J., Östlin, G., Fynbo, J. P. U., et al. 2005 [[arXiv:astro-ph/0506686](https://arxiv.org/abs/astro-ph/0506686)]
- Sokolov, V. V., Fathkullin, T. A., Castro-Tirado, A. J., et al. 2001, *A&A*, 372, 438
- Stanek, K. Z., Matheson, T., Garnavich, P. M., et al. 2003, *ApJ*, 591, L17
- Taylor, G. B., Frail, D. A., & Kulkarni, S. R. 2001, *GCN*, 1136
- van Dokkum, P. G., & Bloom, J. S. 2003, *GCN*, 2380
- Yamazaki, R., Ioka, K., & Nakamura, T. 2002, *ApJ*, 571, L31
- Zeh, A., Klose, S., & Hartmann, D. H., *ApJ* 2004, 609, 952